Photoacoustics 13 (2019) 46–52

Contents lists available at ScienceDirect

Photoacoustics

journal homepage: www.elsevier.com/locate/pacs

Research article

In vivo tracking of orally-administered particles within the gastrointestinal tract of murine models using multispectral optoacoustic tomography

Neal Bhutiani[a,b], Abhilash Samykutty[c], Kelly M. McMasters[a], Nejat K. Egilmez[b], Lacey R. McNally[c,*]

[a] Department of Surgery, University of Louisville, Louisville, KY, 40202, United States
[b] Department of Microbiology and Immunology, University of Louisville, Louisville, KY, 40202, United States
[c] Department of Cancer Biology, Wake Forest School of Medicine, Winston-Salem, North Carolina, 27101, United States

ARTICLE INFO

Keywords:
Multispectral optoacoustic tomography
Gastrointestinal tract
Colon
Oral gavage
Nanoparticle tracking
Diagnostic imaging

ABSTRACT

While particle carriers have potential to revolutionize disease treatment, using these carriers requires knowledge of spatial and temporal biodistribution. The goal of this study was to track orally administered particle uptake and trafficking through the murine gastrointestinal (GI) tract using multispectral optoacoustic tomography (MSOT).

Polylactic acid (PLA) particles encapsulating AlexaFluor 680 (AF680) dye conjugated to bovine serum albumin (BSA) were orally gavaged into mice. Particle uptake and trafficking were observed using MSOT imaging with subsequent confirmation of particle uptake via fluorescent microscopy. Mice treated with PLA-AF680-BSA particles exhibited MSOT signal within the small bowel wall at 1 and 6 h, colon wall at 6, 12, and 24 h, and mesenteric lymph node 24 and 48 h. Particle localization identified using MSOT correlated with fluorescence microscopy. Despite the potential of GI tract motion artifacts, MSOT allowed for teal-time tracking of particles within the GI tract in a non-invasive and real-time manner.

Future use of MSOT in conjunction with particles containing both protein-conjugated fluorophores as well as therapeutic agents could allow for non-invasive, real time tracking of particle uptake and drug delivery

1. Introduction

In both colorectal cancer and inflammatory bowel disease, effective, orally administered therapies represent the ideal route of drug delivery due to ease of administration and patient preference. Particularly in the case of immunomodulatory therapies, however, poor bioavailability and degradation by gastrointestinal enzymes prevents such administration from being more widely utilized. Additionally, noninvasively yet accurately imaging both gastrointestinal cancers and inflammatory bowel disease has proven difficult due to issues with resolution and reliance on grossly detectable differences in tissue density and vascularity.

The development of micro- and nano-based carriers over the last twenty years represents an exciting mechanism to overcome these obstacles. Several studies have demonstrated the potential utility of orally administered therapeutic particles for treatment gastrointestinal (GI) diseases. [1–5] While these molecules demonstrate mucoadhesive properties, which allow their binding to and uptake by the intestinal mucosa before subsequent trafficking to the mesenteric lymph nodes [1], as well as stability in a variety of physiologic environments [2–9], it is essential to track the biodistribution of these delivery vehicles within the gastrointestinal tract in a longitudinal manner to progress these treatments into clinical trials. As previous studies have demonstrated, novel imaging modalities have provided important insight into understanding the trafficking and behavioral characteristics of these agents *in vivo*, including their durability and content (i.e. drug) delivery to target tissues. [10–14] Understanding the time course of particle uptake and localization could facilitate rational therapeutic applications and dosing schema in human subjects.

Multispectral optoacoustic tomography (MSOT) has recently emerged as a high resolution, non-invasive *in vivo* imaging modality. To date, optoacoustic imaging has largely identified solid tumors, namely melanoma, breast cancer, and pancreatic ductal adenocarcinoma, and various aspects of vascularity. [15–21] As MSOT does not require exposure to radiation and nephrotoxic contrast agents, it represents a significant improvement in resolution compared to conventional

* Corresponding author at: Associate Professor Department of Cancer Biology, Department of Bioengineering, Wake Forest School of Medicine, Winston-Salem, NC, 27157, United States.
E-mail address: Lacey_mcnally@hotmail.com (L.R. McNally).

https://doi.org/10.1016/j.pacs.2018.11.003
Received 28 June 2018; Received in revised form 16 October 2018; Accepted 13 November 2018
Available online 17 November 2018

imaging modalities (e.g. computed tomography (CT), magnetic resonance imaging (MRI), ultrasound (U/S)) heightening its appeal as a tool for diagnosis and monitoring of various pathologies. While optoacoustic imaging has been utilized to track biodistribution of nanoparticles injected iv in the context of various cancers [14,22–25], unlike other solid organs, accurately imaging the gastrointestinal tract using MSOT has proven difficult owing to the motility of the small bowel and colon in conjunction with motion artifact introduced by murine respiration.

Our group has worked extensively with biodegradable polylactic acid particles for use in both intravenous and oral immunotherapy delivery. [1–6,8,26] Furthermore, we have recently described high resolution imaging of the gastrointestinal tract using MSOT [27]. This study aimed to evaluate the biodistribution and longitudinally track particle uptake through the murine GI tract *in vivo* after oral administration.

2. Methods

2.1. Orally delivered particles

Polylactic acid particles containing either bovine serum albumin (BSA), BSA conjugated to AlexaFluor 680 dye, or BSA conjugated to AlexaFluor 594 dye were synthesized using a PIN as described previously. [2] Briefly, BSA (Sigma Chemical Co., St. Louis, MO) or BSA-AF680 and PLA (Mr 24,000 and Mr 2000; 1:1 (w/w)], Birmingham Polymers, Inc, Birmingham, AL) were suspended in methylene chloride (Fisher Scientific, Hampton, NH) before being quickly poured into petroleum ether (Fisher) in order to form particles. After formation, solvent was removed by particle filtration and lyophilization overnight. Polylactic acid particles containing BSA-AF680 were diluted in Milli-Q water and characterized using dynamic light scattering and transmission electron microscopy. Multiple batches of particles were constructed to compare the repeatability of particle construction. Additionally, optical density of particles was measured using a spectrophotometer prior to drawing them into the gavage needle as well as after the particles were expelled from the needle. As less than 0.0001 change in OD was observed, we determined that the particles easily passed through at 24 gauge oral gavage needle. The encapsulation efficiencies for the BSA, BSA-AF680, or BSA-AF594 were extrapolated from the measurements of total protein encapsulated into the particles.

2.2. Signal assessment ex vivo in tissue phantoms

To assess the ability of MSOT to detect AF-680 containing particles (hereafter PLA-BSA-AF680), PLA-BSA-AF680 was added to tissue phantoms designed to simulate optical properties of murine tissue. The tissue phantom was constructed by following procedures: Fixed cylindrical phantoms of 2 cm diameter were prepared using a gel made from distilled water containing Agar (Sigma Aldrich, St. Louis, MO, USA) for jellification (1.3% w/w) and an intralipid 20% emulsion (Sigma Aldrich, St. Louis, MO, USA) for light diffusion (6% v/v), resulting in a gel presenting a reduced scattering coefficient of $\mu'^{s} \approx 10\,cm^{-1}$. Blank PLA particles, PLA-BSA-AF60, or BSA-AF680 samples were inserted into cylindrical inclusions approximately 3 mm diameter. The gel used to construct the tissue phantom was used to seal the samples in the appropriate well prior to MSOT imaging

MSOT imaging of the phantoms was done at a single position located approximately in the middle of the phantom. Data acquisition was performed at wavelengths of 680, 710, 730, 740, 760, 770, 780, 800, 850, 900 nm, using 10 averages per wavelength resulting in 1 s acquisition time per wavelength. Signal was measured using a Region of Interest method from MSOT images. Data obtained in MSOT arbitrary units (a.u.) was statistically compared using ANOVA.

2.3. Mice and particle delivery

Balb/c mice were placed on a low anthacyanin, casein-based diet for 48–72 h prior to particle administration. They were then orally gavaged with and equal admixture of PLA-BSA-AF680 (10 μg AF680-BSA/1 mg particles) and PLA-BSA-AF594 (10 μg AF594-BSA/1 mg particles) suspended in phosphate buffered saline (PBS) or an equal admixture of naked AF680-BSA (hereafter BSA-AF680) and AF-594-BSA (hereafter BSA-AF594) suspended in PBS. This was done to allow for particle visualization using both MSOT and fluorescent microscopy, as AF680 was detectable by MSOT but not fluorescence microscopy at our institution, and AF594 was detectable by fluorescence microscopy but not MSOT. Mice each received a total of 5 mg of PLA-BSA-AF680 + 5 mg PLA-BSA-AF594 in 100 μL PBS or 50 μg BSA-AF680 + 50 μg BSA-AF594 suspended in 100 μL PBS. After hair removal using Nair with aloe (Church & Dwight Co., Inc., New Jersey, USA), mice were imaged using multispectral optoacoustic tomography.

2.4. Multispectral optoacoustic tomography

Multispectral optoacoustic tomographic (MSOT) imaging was performed as previously described. Briefly, after anesthesia with 1.6% isofluorane, mice were prepared for imaging using a combination of manual shaving and Nair cream with aloe (Church and Dwight Co., Princeton, NJ, USA) [28]. Mice were subsequently imaged using the MSOT system InVision TF 256 (iThera Medical, Munich, Germany) using wavelengths of 680, 710, 730, 740, 760, 770, 780, 800, 850, and 900 nm with 25 averages per wavelength and an acquisition time of 10 μs per frame. The water temperature was 35 °C within the instrument during acquisition.

2.5. MSOT image reconstruction and analysis

Raw data obtained with MSOT was reconstructed with multispectral analysis performed as previously described [19,29]. Spectral analysis was performed at wavelengths corresponding to deoxy-hemoglobin and BSA-680. Reconstruction was conducted using backprojection at a resolution of 75 μm using ViewMSOT software version 3.5 (iThera Medical, Munich, Germany). The Multispectral Processing was conducted using Linear Regression with ViewMSOT 3.5, where known molar absorptivity spectra (e.g. for oxy-hemoglobin, deoxy-hemoglobin, and nanoparticle) are used to model the relationship between chromophore concentration and MSOT signal over a range of wavelengths. The approach assumes knowledge about all absorbers present in the imaged tissue in order to correctly attribute contributions from the different wavelengths to the unmixed component images[30]. In order to ensure comparability among data sets, the reconstruction parameters (field of view, speed of sound, pixel size, and the high/low pass filters) and spectral unmixing parameters were consistently applied to all data. Spectral unmixing was performed in the absence of correction for fluence heterogeneities and attenuation as a function of tissue depth including spectral coloring. The location of organs was identified based upon vascular pattern. In addition, a region of interest (ROI) method was applied to determine signal strength in the liver, small bowel, colon, spleen, and mesenteric lymph nodes (MLN) of mice acquired at 1 min, 1 h, 6 h, 12 h, 24 h, and 48 h post-gavage using ViewMSOT software and reported as MSOT a.u. The ROI was manually created with an ellipse drawing tool using the deoxy-hemoglobin spectrally unmixed component as a guide for organ location. The ROI area was kept constant for all image slices 3.5 mm^2, thus creating a non-uniform elliptical prism volume of interest (VOI). The mean pixel intensity per cross-section in the VOI for the spectrally unmixed injected agent (BSA-680) was plotted as MSOT signal vs. position to assess the particle location. The maximal 'mean signal per cross-section' in the volume was used as a quantitative indicator of particle trafficking. Since optoacoustic signals using the detection geometry of this system are subject to out-of-

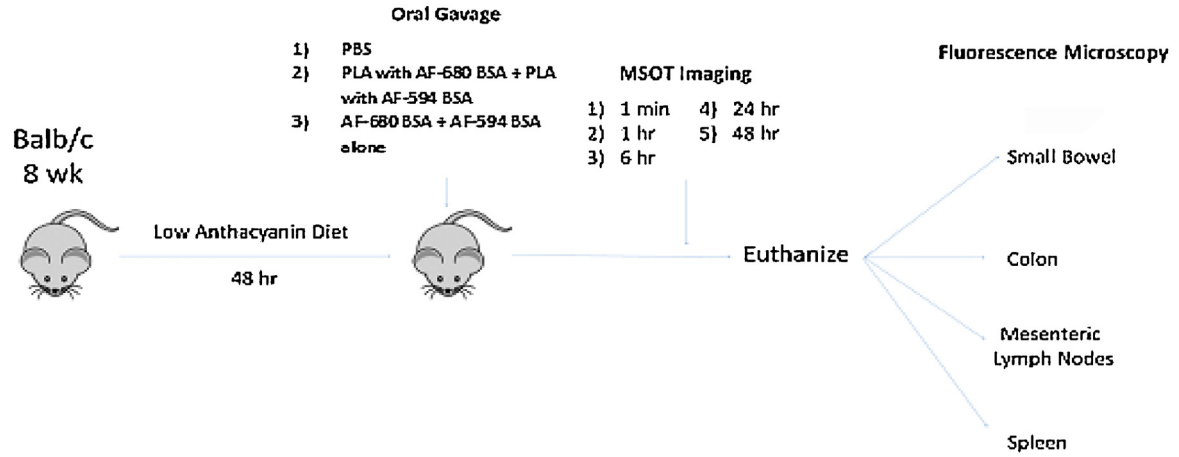

Fig. 1. Experimental Schematic for mouse experiments.

plane contributions, this method was used to find the center of signal intensity and minimize variability from out-of-plane artifacts. The capacity of this optoacoustic system to deliver semi-quantitative data reflective of relative probe accumulation *in vivo* in murine models using the aforementioned reconstruction and multispectral unmixing methods was previously established. [31,32] The MSOT a.u. values for the particle containing BSA-680 were compared using SAS 9.3 (Cary, NC, USA).

2.6. Organ histology and microscopy

After imaging, mice were euthanized and abdominal organs were embedded in paraffin and sectioned at 6 μm thickness, and stained with hematoxylin and eosin (H&E) for evaluation using fluorescence microscopy. Images were acquired using both conventional white light and fluorescence lamps. MSOT images were correlated with fluorescence microscopy images to determine accuracy of MSOT based particle localization. For an experimental schematic, please see Fig. 1.

3. Results

PLA particles were characterized as to size, polydispersity index, and ability to encapsulate BSA-680. As is characteristic of the discrepancy between TEM and DLS particle sizing, PLA particles averaged 33 nm using TEM and 46 nm using DLS (Figs. 2A-B). The generation of 3 batches of PLA-BSA-680 particles also resulted in similar sizing results along with similar polydispersity index of 0.11-0.14 (Fig. 2C). Further comparison of the spectral signature of AF-680 and BSA-680 indicated very little spectral differences (Fig. 2D). Assessment of particles in agar and intralipid tissue phantoms demonstrated that blank PLA particles produced no signal at any excitation wavelength (Fig. 3). PLA-BSA-AF680 produced MSOT signal with intensity 32 MSOT a.u. This was slightly less intense than but otherwise similar to the signal produced by AF680 of 38 MSOT a.u. (Fig. 3).

In *in vivo* studies, mice treated with PLA- BSA-AF680 exhibited MSOT signal in the wall of the small bowel at starting at 1 h after gavage up through 24 h after gavage, in the wall of the colon at 6, 12, and 24 h, in the MLN 12 and 24 h, and in the limited signal in the spleen 48 h. No signal was detected in the liver. Maximum signal post-gavage was noted in the wall of the small bowel at 6 h, colon at 24 h, and MLN at 48 h (Fig. 4). Fig. 5 demonstrate the signal noted in each respective organ at 24 h after gavage. Intralumenal and intraepithelial signal were differentiated through overlay of AF-680 signal on deoxyhemoglobin signal. Mean MSOT signal intensity in target organs at each timepoint corresponded with the visualized signal intensity (e.g. 24 h, Fig. 5). Additional secondary confirmation of PLA-BSA-AF680 signal or BSA-AF680 alone was observed in ex vivo organs, liver, spleen and intestine using near infrared fluorescent imaging after 6 h post gavage (Sup Fig. 2).

Compared to mice gavaged with PLA-BSA-AF680, those gavaged with BSA-AF680 demonstrated similar a much shorter duration of signal visibility on MSOT with very little signal detected after 1 h (Fig. 4), no signal detected after 6 h (Sup Fig. 2), and decreased signal in target tissues. BSA-AF680 was detected immediately following gavage (data not shown) and progressed through the lumen of the gastrointestinal tract with minimal signal noted in the wall of the small bowel and colon at 1 h post gavage and no signal noted in the spleen or liver. BSA-AF680 was not detected by the 6 h timepoint or thereafter.

Particle localization on MSOT correlated well with findings on fluorescence microscopy, which demonstrated particle localization in organs identified on MSOT at each given timepoint (e.g. 24 h, Fig. 6). Specifically, particle uptake was visualized at the apical aspect of epithelial cells in the small bowel and colon and in the MLNs. BSA-AF680 was visualized around splenic sinusoids at the timepoints when signal was observed on MSOT.

4. Discussion

Here, we describe high-resolution imaging of the murine gastrointestinal tract and histologically correlated, site-specific uptake of poly-lactic acid particles by cells in tissues along the gastrointestinal tract. To our knowledge, this represents the first description of such high resolution MSOT imaging of the murine gastrointestinal tract, specifically that which allows for tracking of orally delivered particles.

To date, high resolution gastrointestinal imaging using MSOT has proven challenging due to a combination of 1) intrinsic gastrointestinal motility, 2) lack of fixed organ position within the abdomen, 3) motion artifact conferred by respiration, and 4) artefactual signal produced by anthacyanins in murine food. Ensuring an adequate level of anesthesia, utilizing a casein-based, low-anthacyanin diet, and, most importantly, acquiring 25 averages per wavelength proved critical to enabling detection of organ specific particle localization in our studies. These techniques have also enabled us to image colitis in a murine model with detection of both general areas of inflammation/hypervascularity and individual blood vessels.[27]

In addition to the MSOT imaging protocol, the mucoadhesive properties of the PLA particles facilitated organ identification and histologic correlation with MSOT imaging. While much of the gavaged fluid-particle mixture passes through the gastrointestinal tract, mucoadhesion enables some of the particles to be retained and taken up by absorptive tissues. The mechanism of uptake remains unclear, but likely occurs via phagocytosis given the size of the particles (46 nm average diameter). The importance of mucosal adhesion is illustrated in comparing BSA-AF680 to PLA-BSA-AF680. The former passes through the

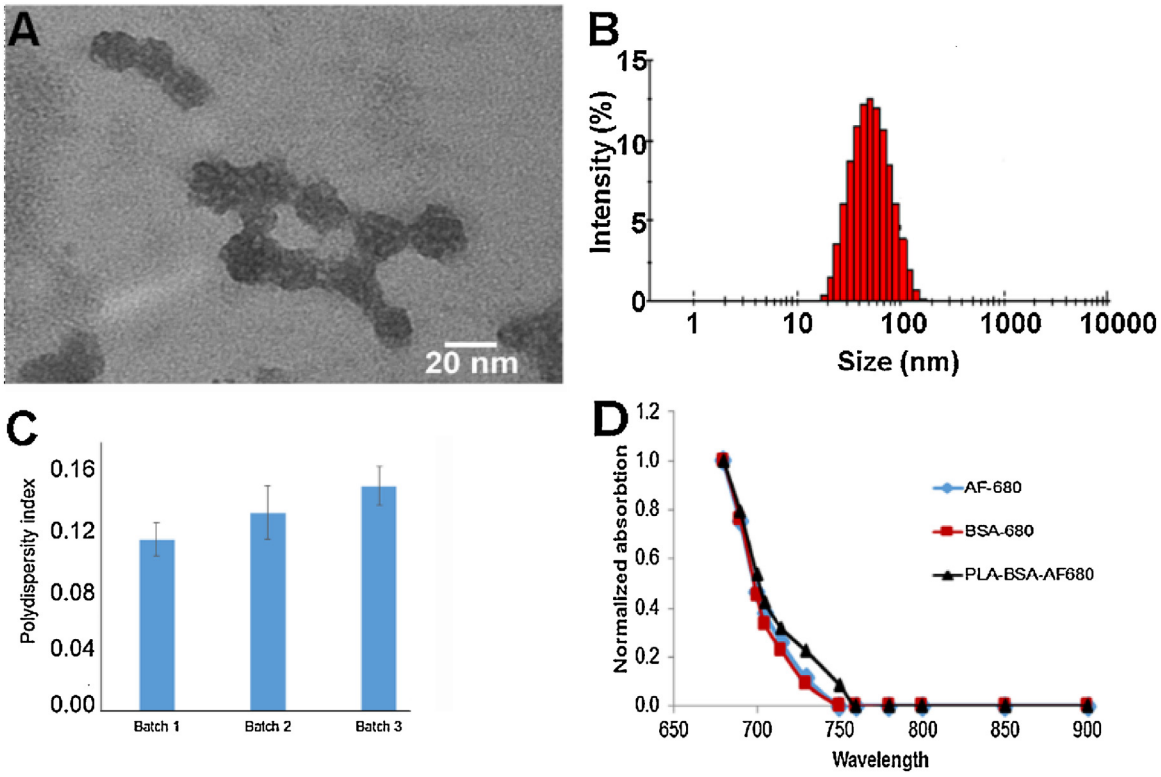

Fig. 2. Characterization of the PLA-BSA-680 nanoparticles. A) Transmission electron micrograph (TEM) images with an average particle size of 33 ± 12 nm. **B)** Dynamic light scattering **(**DLS) of the PLA particles resulted in an average size of 44 nm. **C)** Polydispersity Index (PDI) shows narrow polydispersed distribution as the PDI ranged from 0.12-0.135 over the course of 3 batches of particles evaluated. **D**) Spectral absorption was determined of AF-680, BSA-680, and PLA-BSA-680 which demonstrated a high degree of similarity.

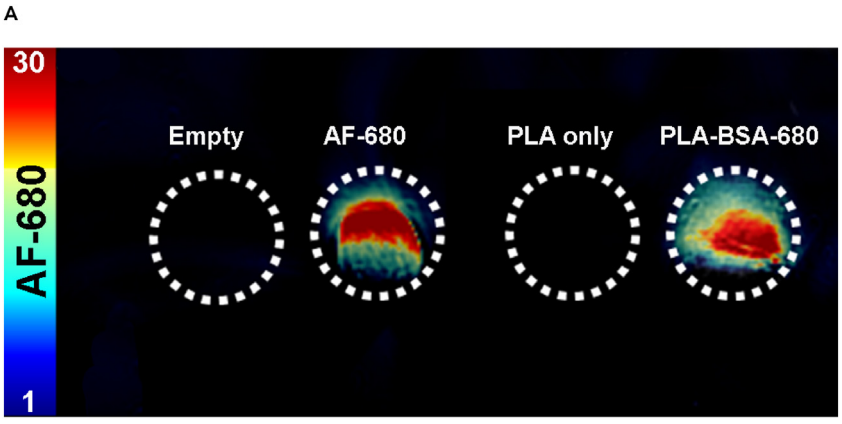

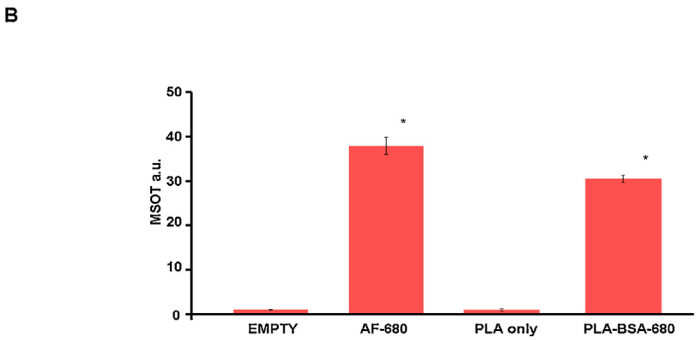

Fig. 3. Evaluation of optoacoustic signal within tissue phantoms of AF-680, PLA only, and PLA-BSA-AF680. (**A**) MSOT signal of AF-680, particles only, and particle-encapsulated AF-680 was determined using the spectral signature in Fig. 2D in tissue phantoms clearly differs from particles alone. (**B**) Uptake of BSA-680 within the PLA particles was demonstrated by similarities of signal intensity between AF-680 and PLA-BSA-680 within tissue phantoms. Both AF-680 and PLA-BSA-680 had significantly higher signal ($p < 0.05$) than PLA only or empty.

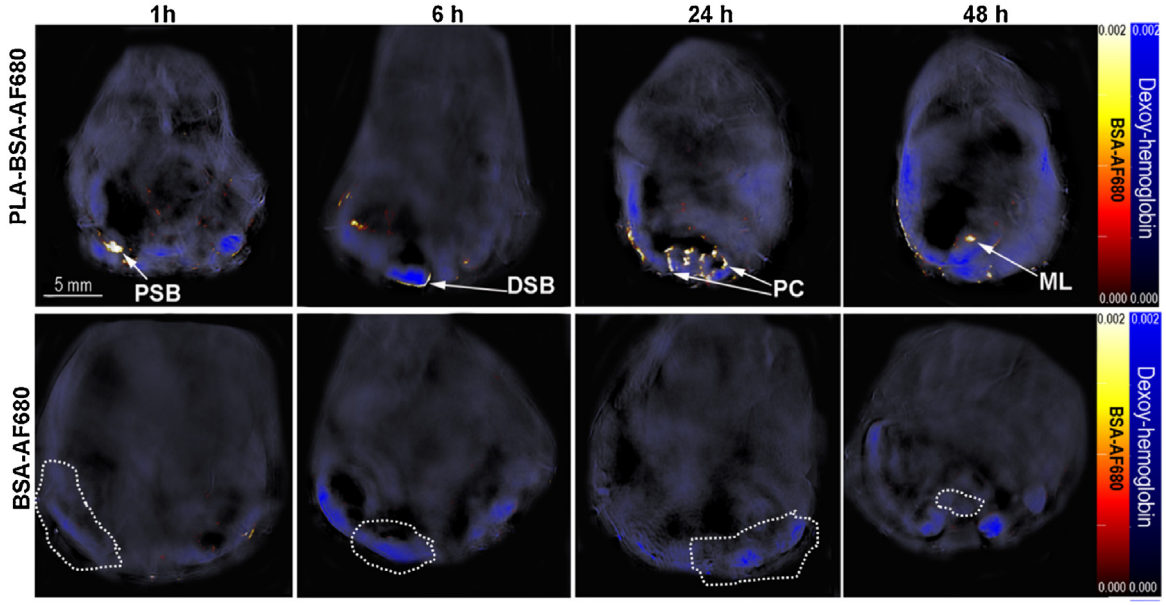

Fig. 4. MSOT signal in gastrointestinal organs after oral gavage of either PLA-BSA-AF680 particles or BSA-AF680 alone. (Top) MSOT imaging demonstrates nanoparticle localization and uptake in the proximal small bowel (PSB), distal small bowel (DSB), proximal colon (PC), and mesenteric lymph node (ML) over the course of 48 h as indicated using arrows. (Bottom) BSA-AF680 was undetectable after 1 h post gavage. Areas of the small bowel, colon, and mesenteric lymph node are circled in the BSA-AF680 treated image. Deoxy-hemoglobin is shown in blue and BSA-AF680 in the hot color bar. All mouse images were equalized to the same intensity scale bar.

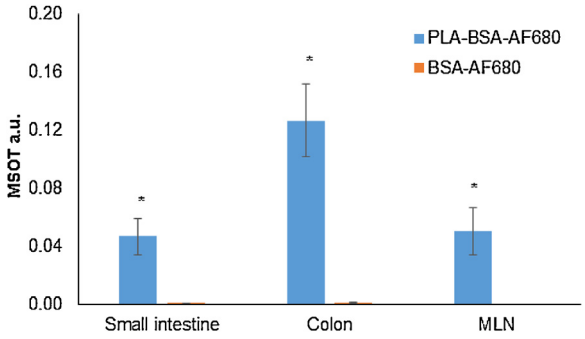

Fig. 5. Mean MSOT signal intensity correlates with particle localization. Data shown here reflects mean MSOT signal intensity of PLA-BSA-680 or BSA-AF680 in colon, small bowel, and MLN 24 h after gavage. Region of interest was determined using a 3.5 mm^2 elliptical region on the assigned area of small intestine, colon, or MLN using View MSOT 3.5. Significantly higher levels of BSA-AF680 were observed in mice that received it via PLA particles than BSA-AF680 alone ($p < 0.001$).

GI tract with minimal absorption, with the small amount of absorption that occurs likely mediated by pinocytosis or passive transport with water uptake. Meanwhile, the latter demonstrates discrete uptake and strong signal on both MSOT (Fig. 4) and histology (Fig. 6).

Indeed, this correlates well with our previous findings that MSOT can reliably detect individual microparticles as small as 75 μm in diameter. [11] Together, the ability of MSOT to detect such small particles as well as its ability to detect fluorophores or other fluorescent contrast agents of various wavelengths present numerous opportunities for clinical imaging applications within the gastrointestinal tract. Of course, use of MSOT can avoid nephrotoxic contrast agents used in conventional imaging modalities such as CT and MRI. However, with the ability to detect multiple fluorophores, MSOT also can allow for particles to be administered orally and intravenously and thus enable simultaneous detection of inflammation, malignancy, and other pathologies. Furthermore, varying particle size, protein or small molecule tags, and biochemical properties (e.g. porosity and pore size, chemical composition, etc.) can allow for tissue specific uptake based on organ or cell type (e.g. tumor cell) [23,28].

While MSOT accurately tracks particle uptake in the gastrointestinal tract and identifies fluorophore signal, it does not readily distinguish between encapsulated and naked fluorophore. For example, we observe signal of similar intensity in the small bowel at 1 h and the proximal colon at 24 h, but the former is produced by encapsulated fluorophore and the latter could indicate either dye containing nanoparticles or dye only. While this does not ostensibly impact imaging using particle-encapsulated fluorophore, it would become important in tracking fluorophore-tagged particles. In the case of PLA particles in this study, it remains unclear at which point the particles are degraded. Discrete particles are observed in the small bowel, colon, and MLN, but not in the spleen. Degradation could be a factor of particle time in circulation, a function of being in the lymphatic circulation, or both. Indeed, previous studies have demonstrated the lymphatic system's role in metabolizing elements of the intercellular matrix and connective tissues (e.g. hyaluronan). [33] Particle-specific studies would be required to determine *in vivo* degradation kinetics, which would in turn impact potential clinical applications.

The findings of this study should be viewed in light of several limitations. All imaging was performed on Balb/c mice, as skin pigment results in signal artifact that prevents high-resolution imaging and would have prevented particle localization. Thus, the present of endogenous skin pigment (e.g. in the case of particularly dark-skin) would limit clinical MSOT utility using a hand-held probe, but would likely not inhibit an endoscopic probe in imaging such patients. Also, MSOT cannot detect non-light absorbing particles, so any clinical application would require incorporation of some absorbing material (e.g. protein conjugated fluorophore, gold) within the nanoparticle. All tissue was fixed in formalin for histology prior to H&E staining. The totality of the processing may have resulted in the loss of some particles in target tissues at each timepoint. Finally, the results presented herein do not necessarily reflect particle content delivery or reflect information regarding the minimum dose of particles that results in detectable MSOT signal in each target organ, but rather, describe the ability to monitor particle travel *in vivo* using MSOT,

Despite these limitations, our findings present a number of

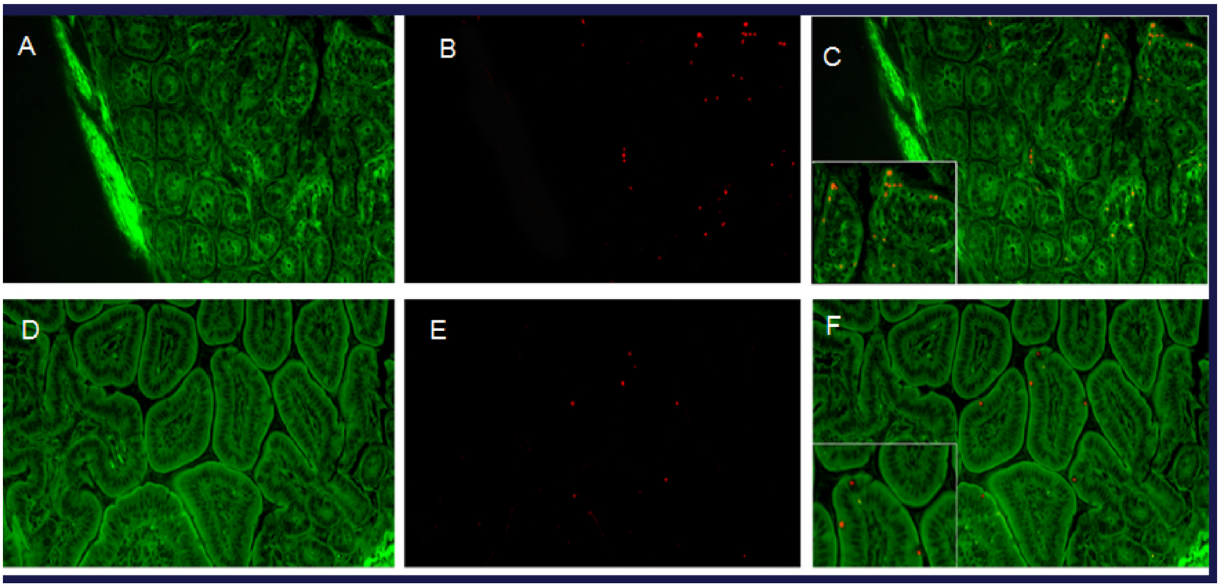

Fig. 6. Histologic visualization of PLA-BSA-AF594. (A–C) demonstrates proximal colon 24 h after oral gavage with PLA-BSA-AF594 (20x), with (C) showing an overlay of particles (red) on intestinal epithelium (green). (D–F) demonstrates small bowel 24 h after oral gavage with particles containing AF-680 (20x), with (F) again showing an overlay of particles (red) on intestinal epithelium (green). Additional images of other organs is located in Supplemental Fig. 3.

opportunities for future investigation. With the recently-developed clinical MSOT apparatus, nanoparticle-tracking studies in the gastrointestinal tract can be replicated in humans to assess the diagnostic utility of MSOT in the clinical setting. Within the last several months, researchers at the University of Erlangen-Nurnberg Medical School demonstrated the ability of MSOT to detect inflammatory changes without exogenous contrast in human subjects. [34] Evaluating MSOT's ability to track fluorophore-containing nanoparticles represents a logical extension of this work. In examining various iterations of particles and dyes, we would be able to correlate particle uptake with enterocolonic inflammation as well evaluate tumor-specific uptake in the setting of enterocolonic malignancy. Finally, using fluorophore-tagged nanoparticles, we could use MSOT to actively track theranostic nanoparticles to actively establish pharmacokinetics of contrast and/or drug delivery.

5. Conclusions

MSOT detects orally administered AF-680 dye encapsulated PLA particles in vivo. These particles demonstrate site-specific uptake in the wall of the small bowel, colon, and mesenteric lymph nodes. MSOT tracking of fluorophore containing particles could improve monitoring of drug delivery and lead to more optimal individualized dosing schedules. Furthermore, with improved specificity, these particles could be further tested in humans in combination with the handheld MSOT to help surgeons identify sites of active disease or malignancy in the operating room.

Conflict of interest

All contributors are associated with the University of Louisville and Wake Forest School of Medicine.

Acknowledgements

This work was supported by NIH grantsR01CA205941, R01EB020125, R01CA212350, and R01CA100656.

Appendix A. Supplementary data

Supplementary material related to this article can be found, in the online version, at doi:https://doi.org/10.1016/j.pacs.2018.11.003.

References

[1] A.Y. Chung, Q. Li, S.J. Blair, M. De Jesus, K.L. Dennis, C. LeVea, J. Yao, Y. Sun, T.F. Conway, L.P. Virtuoso, N.G. Battaglia, S. Furtado, E. Mathiowitz, N.J. Mantis, K. Khazaie, N.K. Egilmez, Oral interleukin-10 alleviates polyposis via neutralization of pathogenic T-regulatory cells, Cancer Res. 74 (19) (2014) 5377–5385.
[2] N.K. Egilmez, Y.S. Jong, Y. Iwanuma, J.S. Jacob, C.A. Santos, F.A. Chen, E. Mathiowitz, R.B. Bankert, Cytokine immunotherapy of cancer with controlled release biodegradable microspheres in a human tumor xenograft/SCID mouse model, Cancer Immunol. Immunother.: CII 46 (1) (1998) 21–24.
[3] N.K. Egilmez, M.O. Kilinc, T. Gu, T.F. Conway, Controlled-release particulate cytokine adjuvants for cancer therapy, Endocr. Metabol. Immune Disord. Drug Targets 7 (4) (2007) 266–270.
[4] M.S. Sabel, J. Skitzki, L. Stoolman, N.K. Egilmez, E. Mathiowitz, N. Bailey, W.J. Chang, A.E. Chang, Intratumoral IL-12 and TNF-alpha-loaded microspheres lead to regression of breast cancer and systemic antitumor immunity, Ann. Surg. Oncol. 11 (2) (2004) 147–156.
[5] A. Sharma, C.M. Harper, L. Hammer, R.E. Nair, E. Mathiowitz, N.K. Egilmez, Characterization of cytokine-encapsulated controlled-release microsphere adjuvants, Cancer Biother. Radiopharm. 19 (6) (2004) 764–769.
[6] N.K. Egilmez, Y.S. Jong, E. Mathiowitz, R.B. Bankert, Tumor vaccination with cytokine-encapsulated microspheres, Lung Cancer (2003) 687–696 Springer.
[7] N.K. Egilmez, Y.S. Jong, M.S. Sabel, J.S. Jacob, E. Mathiowitz, R.B. Bankert, *In situ* tumor vaccination with Interleukin-12-encapsulated biodegradable microspheres: induction of tumor regression and potent antitumor immunity, Cancer Res. 60 (14) (2000) 3832–3837.
[8] T. Gu, M. De Jesus, H.C. Gallagher, T.P. Burris, N.K. Egilmez, Oral IL-10 suppresses colon carcinogenesis via elimination of pathogenicCD4(+) T-cells and induction of antitumor CD8(+) T-cell activity, Oncoimmunology 6 (6) (2017) e1319027.
[9] E. Mathiowitz, J.S. Jacob, Y.S. Jong, G.P. Carino, D.E. Chickering, P. Chaturvedi, C.A. Santos, K. Vijayaraghavan, S. Montgomery, M. Bassett, C. Morrell, Biologically erodable microspheres as potential oral drug delivery systems, Nature 386 (1997) 410.
[10] H.P. Babcock, C. Chen, X. Zhuang, Using single-particle tracking to study nuclear trafficking of viral genes, Biophys. J. 87 (4) (2004) 2749–2758.
[11] N. Bhutiani, C.W. Kimbrough, N.C. Burton, S. Morscher, M. Egger, K. McMasters, A. Woloszynska-Read, A. El-Baz, L.R. McNally, Detection of microspheres in vivo using multispectral optoacoustic tomography, Biotech. Histochem. 92 (1) (2017) 1–6.
[12] M. Lu, X. Cheng, J. Jiang, T. Li, Z. Zhang, C. Tsauo, Y. Liu, Z. Wang, Dual-modal photoacoustic and magnetic resonance tracking of tendon stem cells with PLGA/iron oxide microparticles in vitro, PLoS One 13 (4) (2018) e0193362.
[13] B.S. Schuster, L.M. Ensign, D.B. Allan, J.S. Suk, J. Hanes, Particle tracking in drug and gene delivery research: state-of-the-art applications and methods, Adv. Drug Deliv. Rev. 91 (2015) 70–91.

[14] M.R. Zeiderman, D.E. Morgan, J.D. Christein, W.E. Grizzle, K.M. McMasters, L.R. McNally, Acidic pH-targeted chitosan capped mesoporous silica coated gold nanorods facilitate detection of pancreatic tumors via multispectral optoacoustic tomography, ACS Biomater. Sci. Eng. 2 (7) (2016) 1108–1120.
[15] N. Beziere, N. Lozano, A. Nunes, J. Salichs, D. Queiros, K. Kostarelos, V. Ntziachristos, Dynamic imaging of PEGylated indocyanine green (ICG) liposomes within the tumor microenvironment using multi-spectral optoacoustic tomography (MSOT), Biomaterials 37 (2015) 415–424.
[16] A. Buehler, E. Herzog, A. Ale, B.D. Smith, V. Ntziachristos, D. Razansky, High resolution tumor targeting in living mice by means of multispectral optoacoustic tomography, EJNMMI Res. 2 (2012) 14.
[17] N.C. Burton, M. Patel, S. Morscher, W.H. Driessen, J. Claussen, N. Beziere, T. Jetzfellner, A. Taruttis, D. Razansky, B. Bednar, V. Ntziachristos, Multispectral opto-acoustic tomography (MSOT) of the brain and glioblastoma characterization, Neuroimage 65 (2013) 522–528.
[18] E. Herzog, A. Taruttis, N. Beziere, A.A. Lutich, D. Razansky, V. Ntziachristos, Optical imaging of cancer heterogeneity with multispectral optoacoustic tomography, Radiology 263 (2) (2012) 461–468.
[19] C.W. Kimbrough, S. Hudson, A. Khanal, M.E. Egger, L.R. McNally, Orthotopic pancreatic tumors detected by optoacoustic tomography using Syndecan-1, J. Surg. Res. 193 (1) (2015) 246–254.
[20] V. Neuschmelting, H. Lockau, V. Ntziachristos, J. Grimm, M.F. Kircher, Lymph node micrometastases and in-transit metastases from melanoma: in vivo detection with multispectral optoacoustic imaging in a mouse model, Radiology 280 (1) (2016) 137–150.
[21] R.P. Mason, Commentary on photoacoustic tomography, J. Nucl. Med. 56 (12) (2015) 1815–1816.
[22] A. Samykutty, W.E. Grizzle, B.L. Fouts, M.W. McNally, P. Chuong, A. Thomas, A. Chiba, D. Otali, A. Woloszynska, N. Said, P.J. Frederick, J. Jasinski, J. Liu, L.R. McNally, Optoacoustic imaging identifies ovarian cancer using a microenvironment targeted theranostic wormhole mesoporous silica nanoparticle, Biomaterials 182 (2018) 114–126.
[23] M.K. Gurka, D. Pender, P. Chuong, B.L. Fouts, A. Sobelov, M.W. McNally, M. Mezera, S.Y. Woo, L.R. McNally, Identification of pancreatic tumors in vivo with ligand-targeted, pH responsive mesoporous silica nanoparticles by multispectral optoacoustic tomography, J. Control. Release 231 (2016) 60–67.
[24] G. Balasundaram, C.J.H. Ho, K. Li, W. Driessen, U.S. Dinish, C.L. Wong, V. Ntziachristos, B. Liu, M. Olivo, Molecular photoacoustic imaging of breast cancer using an actively targeted conjugated polymer, Int. J. Nanomed. 10 (2015) 387–397.
[25] K.A. Homan, M. Souza, R. Truby, G.P. Luke, C. Green, E. Vreeland, S. Emelianov, Silver nanoplate contrast agents for in vivo molecular photoacoustic imaging, ACS Nano 6 (1) (2012) 641–650.
[26] T.F. Conway, L. Hammer, S. Furtado, E. Mathiowitz, F. Nicoletti, K. Mangano, N.K. Egilmez, D.L. Auci, Oral delivery of particulate transforming growth factor Beta 1 and all-trans retinoic acid reduces gut inflammation in murine models of inflammatory bowel disease, J. Crohns Colitis 9 (8) (2015) 647–658.
[27] N. Bhutiani, W.E. Grizzle, S. Galandiuk, D. Otali, G.W. Dryden, N.K. Egilmez, L.R. McNally, Noninvasive imaging of colitis using multispectral optoacoustic tomography, J. Nucl. Med. 58 (6) (2017) 1009–1012.
[28] C.W. Kimbrough, A. Khanal, M. Zeiderman, B.R. Khanal, N.C. Burton, K.M. McMasters, S.M. Vickers, W.E. Grizzle, L.R. McNally, Targeting acidity in pancreatic adenocarcinoma: multispectral optoacoustic tomography detects ph-low insertion peptide probes in vivo, Clin. Cancer Res. 21 (20) (2015) 4576–4585.
[29] S.V. Hudson, J.S. Huang, W. Yin, S. Albeituni, J. Rush, A. Khanal, J. Yan, B.P. Ceresa, H.B. Frieboes, L.R. McNally, Targeted noninvasive imaging of EGFR-expressing orthotopic pancreatic cancer using multispectral optoacoustic tomography, Cancer Res. 74 (21) (2014) 6271–6279.
[30] S. Tzoumas, N. Deliolanis, S. Morscher, V. Ntziachristos, Un-mixing molecular agents from absorbing tissue in multispectral optoacoustic tomography, IEEE Trans. Med. Imaging (2013).
[31] S. Morscher, W.H. Driessen, J. Claussen, N.C. Burton, Semi-quantitative Multispectral Optoacoustic Tomography (MSOT) for volumetric PK imaging of gastric emptying, Photoacoustics, Germany (2014) 103–110.
[32] L.R. McNally, M. Mezera, D.E. Morgan, P.J. Frederick, E.S. Yang, I.E. Eltoum, W.E. Grizzle, Current and emerging clinical applications of multispectral optoacoustic tomography (MSOT) in oncology, Clin. Cancer Res. 22 (14) (2016) 3432–3439.
[33] J.R. Fraser, W.G. Kimpton, T.C. Laurent, R.N. Cahill, N. Vakakis, Uptake and degradation of hyaluronan in lymphatic tissue, Biochem. J. 256 (1) (1988) 153–158.
[34] M.J. Waldner, F. Knieling, C. Egger, S. Morscher, J. Claussen, M. Vetter, C. Kielisch, S. Fischer, L. Pfeifer, A. Hagel, R.S. Goertz, D. Wildner, R. Atreya, D. Strobel, M.F. Neurath, Multispectral optoacoustic tomography in Crohn's disease: noninvasive imaging of disease activity, Gastroenterology 151 (2) (2016) 238–240.

Dr. Neal Bhutiani, is a general surgery resident at the University of Louisville School of Medicine. He graduated from Johns Hopkins University School of Medicine in 2013, after which he began his training in general surgery at the University of Louisville. Dr. Bhutiani is currently working towards his pH.D. in immunology and intends to apply for fellowship and pursue a career in surgical oncology after completing his residency.

Abhilash Samykutty, is currently a postdoctoral researcher at the Wake Forest Baptist Comprehensive Cancer Center, NC, USA. He completed his pH.D. in Medical Biochemistry at UIC, USA/MUHS, India in 2014. His current research interests include synthesis and characterization of the nanoparticles, development of the drug delivery systems and photoacoustic imaging.

Dr. Nejat Egilmez, currently holds the position of Chairman in the Department of Microbiology and Immunology, School of Medicine, University of Louisville. He has led an independent research program since 2001 focusing on the study of tumor immunity, immune therapy and immune regulation. His research program entails two major projects. The first aims to delineate the role of homeostatic T-cell regulatory mechanisms in controlling post-therapy antitumor T-effector cell activity in cancer therapy. The second looks to elucidate the link between chronic inflammation and tumorigenesis.

Kelly M. McMastersMD, PhD, is the Ben A. Reid, Sr., MD Professor and Chair of the Hiram C. Polk, Jr., MD Department of Surgery at the University of Louisville School of Medicine, where he also serves as Director of the Multidisciplinary Melanoma Clinic and Associate Director of the J. Graham Brown Cancer Center, Louisville, KY. His laboratory has focused on cancer gene therapy and melanoma biomarkers, and has been funded by the American Cancer Society, the National Institutes of Health, and the Melanoma Research Foundation, among other agencies. He holds two patents for his research inventions. He is the author and Principal Investigator of the Sunbelt Melanoma Trial, a multi-institutional study involving over 3500 patients from 79 institutions across North America. Dr. McMasters is currently President of the Western Surgical Association, President-Elect of the Society of Surgical Oncology, Vice-president of the Society of Surgical Chairs, and Secretary of the Southern Surgical Association. He is a former President of the Southeastern Surgical Congress. He served on the Melanoma Staging Committee of the American Joint Commission on Cancer (AJCC) and is currently Deputy Editor of *Annals of Surgical Oncology*.

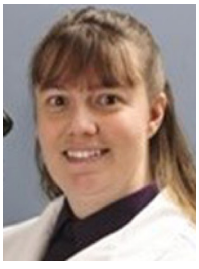

Lacey R. McNally PhD, is an Associate Professor in the Departments of Cancer Biology and Bioengineering at the Wake Forest School of Medicine, Winston-Salem, NC, USA. Dr. McNally was the first to utilize MSOT technology for abdominal tumor detection within the USA. Her laboratory focuses on the development of disease targeted small molecules and nanovehicles that are detectable using MSOT and NIR fluorescent imaging.